Development of Toroidal Nanostructures by Self-Assembly: Rational Designs and Applications

YONGJU KIM,[†] WEN LI,[†] SUYONG SHIN,[‡] AND MYONGSOO LEE*,[†]

[†]State Key Lab of Supramolecular Structure and Materials, College of Chemistry, Jilin University, Changchun 130012, China, and [‡]Department of Chemistry, Seoul National University, Seoul 151-747, Korea

CONSPECTUS

Toroidal nanostructures are symmetrical ring-shaped structures with a central internal pore. Interestingly, in nature, many transmembrane proteins such as β-barrels and α-helical bundles have toroidal shapes. Because of this similarity, toroidal nanostructures can provide a template for the development of transmembrane channels. However, because of the lack of guiding principles for the construction of toroids, researchers have not widely studied the self-assembly of toroidal nanostructures as compared with the work on other supramolecular architectures.

In this Account, we describe our recent efforts to construct toroidal nanostructures through the self-assembly of rationally designed building blocks. In one strategy for building these structures, we induce interfacial curvatures within the building blocks. When we laterally graft a bulky hydrophilic segment onto a p-oligophenyl rod or β-sheet peptides, the backbones of the self-assembled structures can bend in response to the steric effect of these large side groups, driving the p-oligophenyl rod or β-sheet peptides to form nanosized toroids. In another strategy, we can build toroids from bent-shaped building blocks by stacking the macrocycles. Aromatic segments with an internal angle of 120° can associate with each other in aqueous solution to form a hexameric macrocycle. Then these macrocycles can stack on top of each other via hydrophobic and $\pi-\pi$ interactions and form highly uniform toroidal nanostructures. We provide many examples that illustrate these guiding principles for constructing toroidal nanostructures in aqueous solution.

Efforts to create toroidal nanostructures through the self-assembly of elaborately designed molecular modules provide a fundamental approach toward the development of artificial transmembrane channels. Among the various toroids that we developed, a few nanostructures can insert into lipid membranes and allow limited transport in vesicles.

Introduction

The construction of well-defined nanostructures by molecular self-assembly through rational design is a major challenge in supramolecular chemistry.[1,2] A variety of supramolecular architectures has been created by thoroughly investigating the self-assembly behavior based on various self-assembling building block amphilphiles.[3−7] The supramolecular architectures have a well-defined size and shape including fibers, ribbons, tubes, helices, cylindrical micelles, vesicles, spherical micelles, bilayers, and toroids.[8−14] Among diverse nanostructures, toroids have a unique annular shape with an internal pore in the central region.[15,16] It shows a short nanotube-like shape with a length of a few nanometers. Interestingly, a structural motif of toroidal nanostructures is
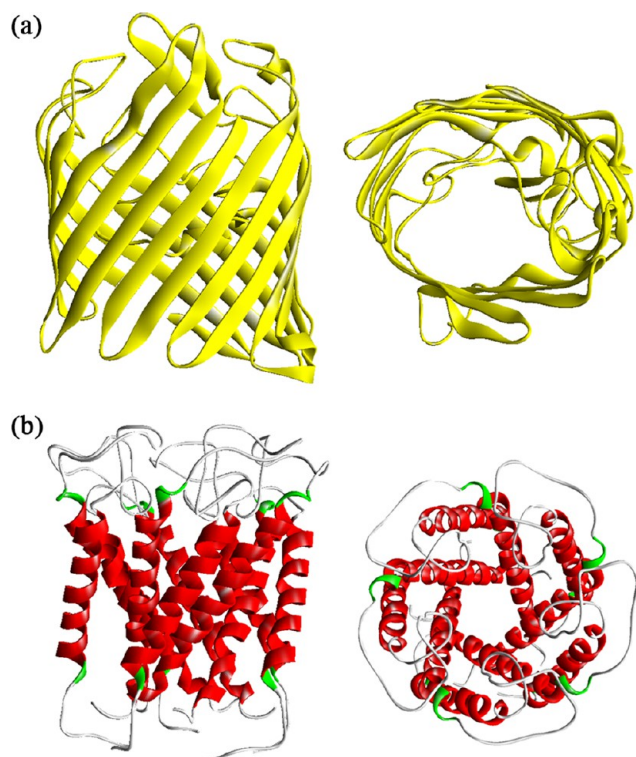
FIGURE 1. Membrane-protein models representing two general categories of a transmembrane-region structure: (a) β-barrel transmembrane region (PDB 1OMF) has a 4.7 nm external diameter and 1.0 nm internal diameter; (b) α-helical transmembrane region (PDB 1MSL) has a 5.0 nm external diameter and 0.9 nm internal diameter.

found commonly in many transmembrane proteins. For example, the β-barrel, which is encountered in the outer membranes of bacteria, mitochondria, and chloroplasts, exhibits a closed β-sheet structure where the first and last β-strands are connected by hydrogen-bonding (Figure 1a).[17] The α-helical transmembrane region is also another example. It contains a bundle of several protein helices that span the membrane and enables specific molecules to be transported across the lipid bilayer (Figure 1b).[18]

On the structural basis of the toroidal nanostructures, several research groups have designed and constructed self-assembled toroids through amphiphilic block copolymers, DNAs, rod–coil amphiphiles, peptides, and proteins.[19–25] However, because of the lack of a guiding principle for the preparation of toroids, self-assembly into the toroidal nanostructure has not been widely studied compared with the other supramolecular architectures such as fibers, micelles, sheets, and vesicles. In recent research, we have studied the construction of toroidal nanostructures through the self-assembly of rigid–flexible amphiphilic molecules and synthetic peptide block molecules. From our work, we can draw following two general principles: the induction of interfacial

curvature or the stacking of the macrocycles. In the interfacial curvature principle, a bulky and hydrophilic flexible segment is placed in the middle of the hydrophobic rigid segments such as p-oligophenyl rods or β-sheet peptides. As a result, curvature at the interface of the building blocks can be induced to decrease steric repulsion between the bulky hydrophilic segments. Finally, the amphiphilic building blocks can self-assemble into highly curved toroidal nanostructures. In another principle, the toroids can be constructed by the stacking of the macrocycles. Bent-shaped aromatic segments with an internal angle of 120° can form hexameric macrocycles at the initial stage. The resulting noncovalent hexameric macrocycles can further stack on top of each other to form highly uniform toroidal nanostructures through hydrophobic and $\pi-\pi$ interactions. Interestingly, slight molecular modifications in the bent-shaped block molecules can lead to the formation of interesting expandable toroids.

With these principles, this Account describes recent research in the development of toroidal nanostructures via rigid–flexible amphiphiles and synthetic peptides. In the later part of the Account, a few toroids are subjected to function as artificial channels because of their unique annular shape with an internal pore in the central region, which is similar to the shape of the transmembrane protein.

Toroidal Nanostructures from Self-Assembly of Rigid–Flexible Amphiphiles

The rigid–flexible amphiphilic small molecules are composed of rigid aromatic segments and flexible coil segments. They can form supramolecular structures with dimensions as small as a few nanometers, which are not common in microphase separated flexible block molecules. Therefore, the rigid–flexible amphiphilies can be excellent candidates for creating well-defined supramolecular architectures such as nanometer-sized toroids.[26] These amphiphilic combination leads to the formation of a nanostructure with a rigid hydrophobic core surrounded by flexible hydrophilic chains in an aqueous solution.[27]

Molecules **1** and **2** have a bis(ethylene glycol) chain and a longer tris(ethylene glycol) chain, respectively, as a flexible hydrophilic segment with the same hydrophobic segment, hepta-p-phenyl group and hydrophobic chain (Figure 2a).[28] In an aqueous solution, molecule **1** self-assembles into planar sheets, whereas molecule **2** forms a ribbon-like nanostructure due to a different volume of hydrophilic chain. For the formation of the toroid, curvature at the interfaces of the amphiphiles was introduced through molecule **3**, which
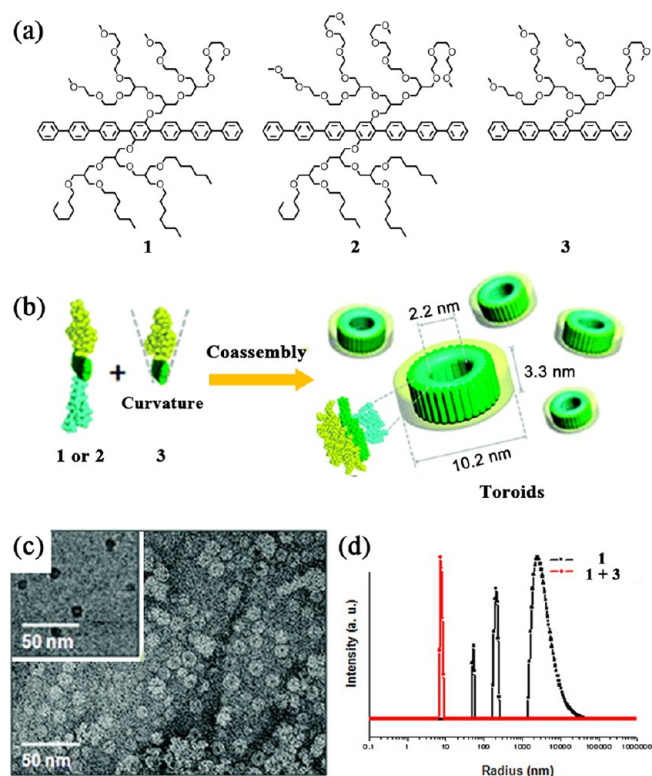
Self-assembled toroids can also be constructed through the stacking of the macrocycles from bent-shaped aromatic segments. Amphiphiles **4** and **5** have an internal angle of 120° from a meta-linked aromatic segment and an oligoether dendron side group (Figure 3).[29,30] The self-assembly of amphiphile **4** leads to the toroidal nanostructure through the formation of hexameric macrocycles. The negatively stained TEM images revealed a light exterior and a dark interior, indicating that the assembled objects are toroid-shaped nanostructures with internal cavities. The toroidal nanostructures were further confirmed by the cryogenic-TEM image as shown in the inset of Figure 3a. The internal and exterior diameters of the toroids are approximately 3 and 8 nm, respectively, showing a highly uniform toroid size that is consistent with the size distribution of DLS result. Finally, the toroids are composed of stacks of several hexameric macrocycles, resulting in a height of approximately 3 nm.

On the basis of the stacking of the macrocyles, we were able to create larger toroids through a slipped packing arrangement, *J*-type stacking. Amphiphile **5** is basically composed of a meta-linked aromatic segment and an oligoether dendron side group and showed a similar structure to that of **4** (Figure 3b).[30] The differences between **4** and **5** are the formyl group, the volume of hydrophilic dendron, the pyridine-linked aromatic segment, and the length of the aromatic segment. The formyl group of **5** led to a weaker intermolecular dipole interaction than that from the cyano group of **4**, and the introduction of the pyridine group induced the formation of water clusters at the nitrogen atom. Because of the weak dipole interaction of the formyl group and the steric repulsion of the water cluster, slipping motion between adjacent aromatic segments could be induced. The spectroscopic results showed that the absorption maximum of **5** in aqueous solution is red-shifted and the fluorescence intensity is apparently enhanced with respect to those observed in chloroform solutions in great contrast to the case of **4** (Figure 3c). These results are indicative of *J*-type stacking of the aromatic segment, suggesting that **5** self-assembled with a slipped packing arrangement in the hexameric macrocycles. Finally, by the self-assembly of **5**, we can construct the larger toroids than those of **4** in aqueous solution. The TEM and AFM experiments clearly showed toroidal objects with a uniform diameter of 11 nm and an internal cavity diameter of 4 nm, which is consistent with the DLS experiment result, 12 nm (Figure 3b,d). In short, we could introduce the *J*-type stacking via the rational design of building blocks and expand both external and internal diameters of the toroids.
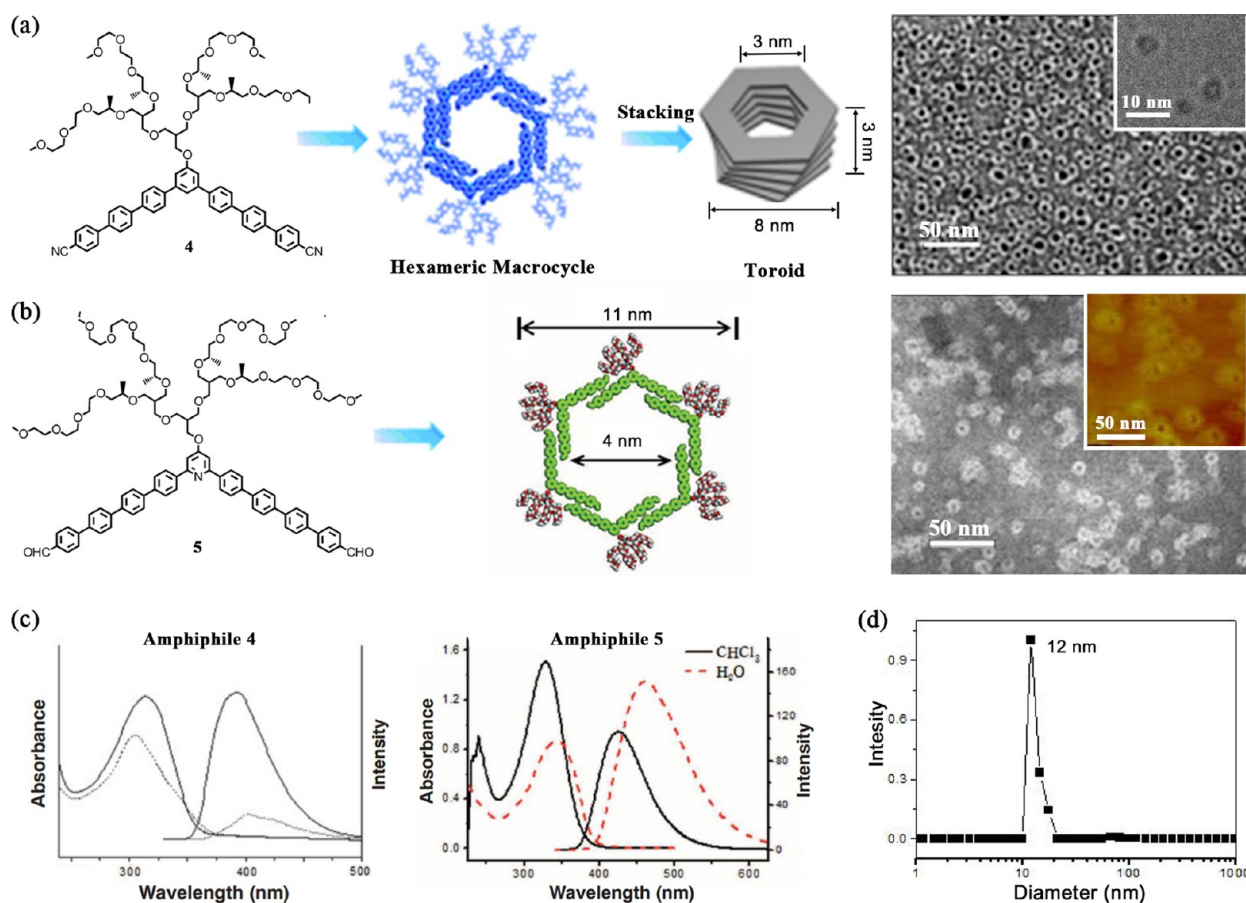

FIGURE 2. (a) Chemical structures of **1**, **2**, and **3**. (b) Schematic illustration of the formation of toroids via the coassembly of **1** or **2** with **3**. (c) TEM image of toroidal nanostructures of **1** containing **3** (90 mol % relative to **1**) in aqueous solution; the inset is a cryo-TEM image of the toroids. (d) Size distribution graphs of **1** and **1** containing **3**. Reprinted with permission from ref 28. Copyright 2009 American Chemical Society.

consists of only a hydrophilic bulky dendron with a lack of hydrophobic chains. When **1** or **2** was coassembled with **3** in aqueous solution, the average hydrodynamic radius (R_H) of both mixed solutions decreased with increasing content of **3** in dynamic light scattering (DLS) experiments (Figure 2d). This indicates a decrease in the size of the aggregates upon the addition of **3**.

The transmission electron microscopy (TEM) image in Figure 2c exhibited the formation of highly curved toroids as a result of the coassembly of **1** and **3**. The diameter of the toroid exterior and the internal pore were measured to be ∼10 and 1.5−2 nm, respectively. The cryogenic-TEM image in the inset of Figure 2c also showed dark toroidal objects against the vitrified solution background. These sizes indicate that the highly curved toroids are composed of a single layer of the molecules in which the hepta-*p*-phenyl rod segments are oriented perpendicularly to the plane of the rings (Figure 2b). Water-soluble toroids with a hydrophobic cavity were formed successfully by the induction of the curvature based on the coassembly of laterally grafted rod amphiphiles.

FIGURE 3. (a) Molecular structure of bent-shaped rod amphiphile **4** and schematic representation of helical stacking of hexameric toroidal macrocycles and negatively stained TEM image. The inset is a cryo-TEM image. Reprinted with permission from ref 29. Copyright 2010 John Wiley and Sons. (b) Molecular structure of bent-shaped rod amphiphile **5** and negatively stained TEM image of **5** from 0.002 wt % in an aqueous solution. The inset is an AFM image on mica. Reprinted with permission from ref 30. Copyright 2012 American Associanation for the Advancement of Science. (c) Absorption and emission spectra of **4** and **5** in CHCl$_3$ (solid line) and an aqueous solution (dashed line). (d) The DLS data, 0.002 wt % of **5** in an aqueous solution.

Toroidal Nanostructures from Self-Assembly of Synthetic Peptide Building Blocks

Peptides are the major molecular scaffolds of the biological world and are made of the same building blocks as proteins. Because the constituents of peptides and amino acids are biocompatible, nanostructures self-assembled from peptide building blocks have received considerable attention as potential sources of engineered bioactive material.[12,16,31−33] Furthermore, the synthetic peptides can have advantages in terms of diverse primary structures, since the basic 20 natural amino acids and endless non-natural amino acids are available as building blocks. There are excellent papers for channel formation based on the synthetic peptide building blocks.[34,35]

Self-assembled β-sheet peptides have attracted a great deal of attention in various research areas. The β-sheet fibrils are organized in such a way that each β-strand is arrayed perpendicularly to the fibril axis. Although the

β-sheet structure has mostly formed one-dimensional (1D) nanostructures, some toroidal structures can be generated as discrete intermediates during the fibrillization of β-amyloid and α-synuclein.[36] Based on these findings, we designed artificial β-sheet peptides that could self-assemble into toroidal nanostructures. The block copolypeptide **6** has a β-sheet forming peptide-based block as a rigid hydrophobic segment and a sugar and a highly charged poly-(L-arginine) block as a hydrophilic segment (Figure 4a).[15] The β-sheet forming peptide block is composed of alternatively placed hydrophobic (tryptophan), positively charged (lysine), and negatively charged (glutamic acid) amino acids. It has been demonstrated that many peptides with a potential to form β-sheet nanofibers often transform into higher order aggregates through lateral hydrophobic interactions. Therefore, we conjugated the hydrophilic poly(ethylene glycol) (PEG) with a peptide segment to inhibit further aggregation by increasing the
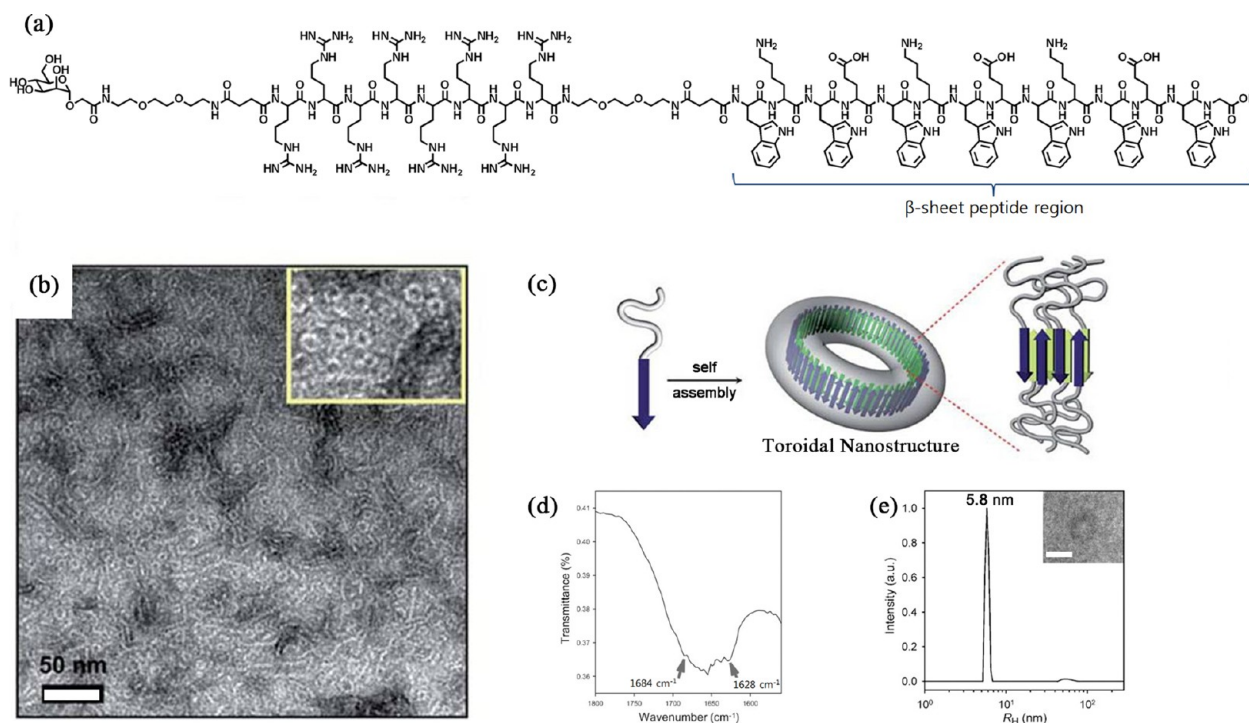
FIGURE 4. (a) The representative chemical structure of block peptide **6** based on poly(L-arginine) and a β-sheet peptide. (b) Negative stained TEM image of **6** in PBS. The inset is a magnified TEM image. (c) Schematic representation of a toroidal nanostructure from **6**. (d) FT-IR spectrum of **6**. Arrows indicate bands at 1684 and 1628 cm^{-1}. (e) DLS analysis of **6**; the inset is a cryo-TEM image (scale bar is 10 nm). Reprinted with permission from ref 15. Copyright 2011 John Wiley and Sons.

solubility of the 1D β-sheet structures. Finally, the rationally designed peptide **6** self-assembled into toroidal nanostructures in aqueous solution. As shown in Figure 4b, discrete toroidal nanostructures were found to coexist with β-ribbon nanostructures. The coexistence of toroids and β-ribbons with the uniform sizes 9.8 ± 0.8 nm in width suggests that toroids are likely to form via end-to-end connections of β-ribbons. The FT-IR spectrum showed two bands at 1684 and 1628 cm^{-1}, the characteristics of antiparallel β-sheet conformation (Figure 4c,d). The DLS analysis revealed that the aggregated objects have a 5.8 nm hydrodynamic radius, and this DLS result was consistent with cryo-TEM data (Figure 4e).

Cyclization of diblock peptides can self-assemble into well-defined nanostructures in aqueous solution by decreasing the conformational entropy. An example is provided by the peptide macrocycle **7**, which consist of an α-helical peptide segment and a β-sheet forming segment (Figure 5).[37] The α-helix-forming segment is based on many alanines and two lysine groups. The lysines are introduced to increase water solubility and to prevent aggregation between α-helix segments. The β-sheet forming segment is a repeat of hydrophobic (tryptophan) and positively (lysine) or negatively (glutamate) charged amino acids as previously mentioned. Oligo(ethylene glycol)-based linker segments are placed

between the α-helix- and β-sheet-forming sequences to decouple both segments. The macrocyclization of synthetic peptides as a key feature was designed under the following hypotheses: (1) a macrocyclization of peptide will partially stabilize the α-helical structure by decreasing the conformational entropy of the unfolded state, and (2) coil-to-rod transition in the β-sheet segment induced by self-assembly will further constrain and stabilize the helical structure. As a result of macrocyclization, we could construct both α-helical structure and β-sheet structure on each building block in the aggregates. Interestingly, because the α-helical peptide segment is bulkier than the β-strand segment, we could induce curvature at the interfaces and the macrocyclic peptide finally self-assembled into toroids. As shown in the negatively stained TEM image of Figure 5, the self-assembly of **7** in aqueous solution could form the toroidal nanostructure successfully. Therefore, the macrocyclic design principle can provide a promising starting point for developing the toroidal nanostructure based on artificial synthetic peptide assembly.

Potential of Toroidal Nanostructures for Artificial Transmembrane Channels

Many artificial transmembrane channels have been investigated,[38−42] and notable examples are described in
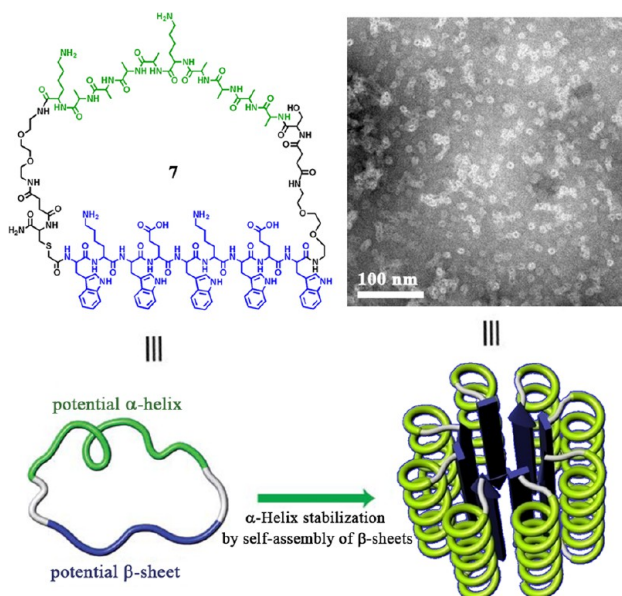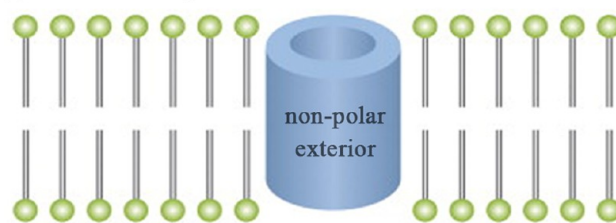
FIGURE 5. Self-assembly of macrocyclic peptides into toroidal nanostructures. Chemical structures of macrocyclic peptide **7**: α-helical segments, green; β-sheet segment, blue; linker, black. Reprinted with permission from ref 37. Copyright 2009 John Wiley and Sons.
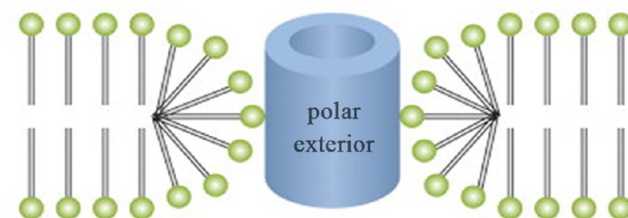

FIGURE 6. Representations of (a) barrel−stave and (b) toroidal pore models. Reprinted with permission from ref 50. Copyright 2008 Elsevier.

p-oligophenyl rod based β-barrel systems,[43,44] β-barrel helical pores from amphiphilic dendritic peptides,[31,45] oligoester based ion channels,[46−48] and β-sheet nanotubes from cyclic peptides.[32] In this section, we introduce the potential of toroidal nanostructures as artificial transmembrane channels.

The synthetic toroids described above are formed in aqueous solution with a hydrophilic exterior. Therefore, one may speculate whether the toroids can function as channels across the hydrophobic lipid membrane environment. However, there are generally two different models, the so-called barrel−stave and toroidal models, for the formation of transmembrane channels based on antimicrobial peptides.[49,50] Many antimicrobial peptides, which contain an abundant and diverse group of molecules that are produced by many tissues and cell types, induce the formation of an aqueous pore across the membrane bilayer by the barrel−stave pore or toroidal pore models. In the barrel−stave model (Figure 6a), peptide helices form a bundle in the bilayer membrane and their hydrophobic portions are placed in contact with the hydrophobic segment of the lipid bilayer. This type of transmembrane channel is induced by alamethicin. Contrastingly, in the toroidal pore model, the hydrophilic part of peptide channels associate with the hydrophilic head groups of the lipids and cause the lipid monolayers at both sides of the membrane to be connected continuously through the pore (Figure 6b). The pore inducing

peptides are amphipathic because the peptides are located at the water−lipid interface in the polar head-groups throughout the channel. Peptides such as magainins, protegrins, melittin, LL-37, and MSI-78 generate this type of transmembrane channel. Based on these models, we predicted that our well-designed toroids with a hydrophilic exterior would be able to function as artificial transmembrane channels by adopting the toroidal model. Indeed, the toroid with hydrophilic exterior functions as proton channels across a lipid bilayer.

The functional toroids can be constructed by self-assembly of rigid−flexible diblock macrocycles. An amphiphilic macrocycle (**8**), consisting of a hexa-*p*-phenyl rod and a PEG flexible coil, self-assembles into toroidal nanostructures with a hydrophilic exterior and interior in bulk and aqueous solution (Figure 7).[51] In the aqueous solution, the hexa-*p*-phenyl rods are aligned axially with their preferred direction, and the interior and exterior are filled by the hydrophilic flexible coil segments. This generates barrel-like supramolecular toroids illustrated in Figure 7c. The average diameter of the toroids was measured to be approximately 7 nm uniformly on the basis of the DLS study and TEM study. The TEM images showed an obvious contrast between the periphery and center of the toroids, which is characteristic of projection images of toroidal nanostructures, and indicated that the diameter of the internal pore was approximately 2 nm (Figure 7b).

The primarily membrane transport activity experiment on **8** was performed with uniformly sized vesicles composed
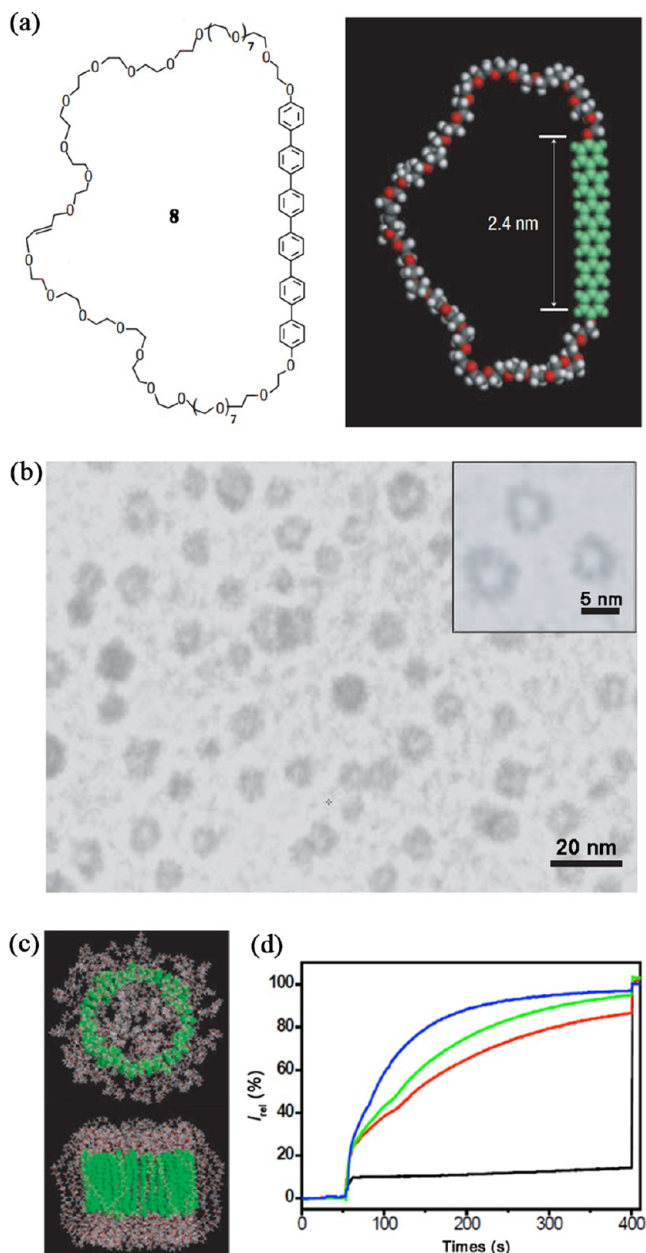
FIGURE 7. (a) Molecular structure of an amphiphilic rigid−flexible macrocycle **8**. (b) TEM image in an aqueous solution. The inset is a higher-magnification image showing the contrast between the periphery and center. (c) Top view and side view of a toroidal nanostructure by molecular modeling of **8** (rod segments are colored green and flexible segments are colored gray). (d) Change in fluorescence intensity at $\lambda_{em} = 510$ nm ($\lambda_{ex} = 450/405$ nm) of vesicle entrapped HPTS with 5 mol % (blue), 2 mol % (green), or 1 mol % of **8** (red) and without **8** (black) as a function of time after addition of 21 μL of a 0.5 M NaOH aqueous solution ($T = 50$ s) and 30 μL of a 5% Triton X-100 aqueous solution ($T = 400$ s). Reprinted with permission from ref 51. Copyright 2005 Nature Publishing Group.

of fresh egg-yolk phosphatidylcholine (EYPC) and cholesterol. The vesicles entrapped a pH-sensitive dye, 8-hydroxypyrene-1,3,6-trisulfonic acid (HPTS), and the emission of the

intravesicular HPTS was monitored after adding the toroidal structures of **8** (Figure 7d). As opposed to the vesicles without **8**, those with **8** showed that the increase in pH resulted in a significant increase of fluorescence intensity, thereby indicating that **8** is membrane-active. Therefore, we could suggest that this self-assembled toroid functions as an artificial transmembrane proton channel primarily, and this may be based on the association of hydrophilic PEG coil with the hydrophilic head groups of the lipids by the toroidal pore model.

As previously described, we hypothesized that the induction of curvature between the adjacent building blocks would form toroidal aggregates with a highly curved structure. On the basis of this hypothesis, we designed an organic/peptide hybrid T-shape building block **9** that consists of a β-sheet forming peptide and an oligo(ethylene oxide) dendron (Figure 8a).[52] Because the steric repulsion of the bulky and hydrophilic dendron in the middle of the peptides induces curvature at the interface between each building blocks, the T-shape molecules can self-assemble into highly curved toroidal nanostructures (Figure 8b). The toroids showed highly uniform diameters (11 nm exterior and 3 nm interior) as shown in negatively stained TEM images and DLS results. The cryo-TEM image also showed dark toroidal objects against the vitrified solution background, confirming that the toroids have been formed in aqueous solution (Figure 8c). The FT-IR spectrum peaks at 1631 and 1691 cm^{-1} revealed that the β-sheet structure had an antiparallel conformation (Figure 8d). Finally, all of these data indicated that the toroids have a single layer of T-shapes building blocks, which consists of an antiparallel β-sheet interior and a hydrophilic oligo(ethylene oxide) dendron exterior, and the β-strands in the toroids are oriented perpendicularly to the plane of the toroids.

An additional T-shaped building block, **10**, was also prepared for application as a transmembrane channel in the lipid bilayer membranes. Molecule **10** had a hydrophobic flexible chain instead of the hydrophilic oligoether dendron to interact with the hydrophobic space of lipid bilayer membranes, as in barrel−stave model. The relative volume fraction of the flexible hydrophobic dendron of **10** was similar to that of **9** to form the optimal curvature. A circular dichroism (CD) spectrum of peptide **10** in only methanol solution did not show the well-defined secondary structures of peptide (Figure 9a, open circle). However, peptide **10** adopted β-sheet conformation within dioleoylphosphatidylcholine (DOPC) liposomes, showing characteristic peaks of β-sheet such as an intense negative minimum of ellipticity at 216 nm, a strong positive maximum at 197 nm,
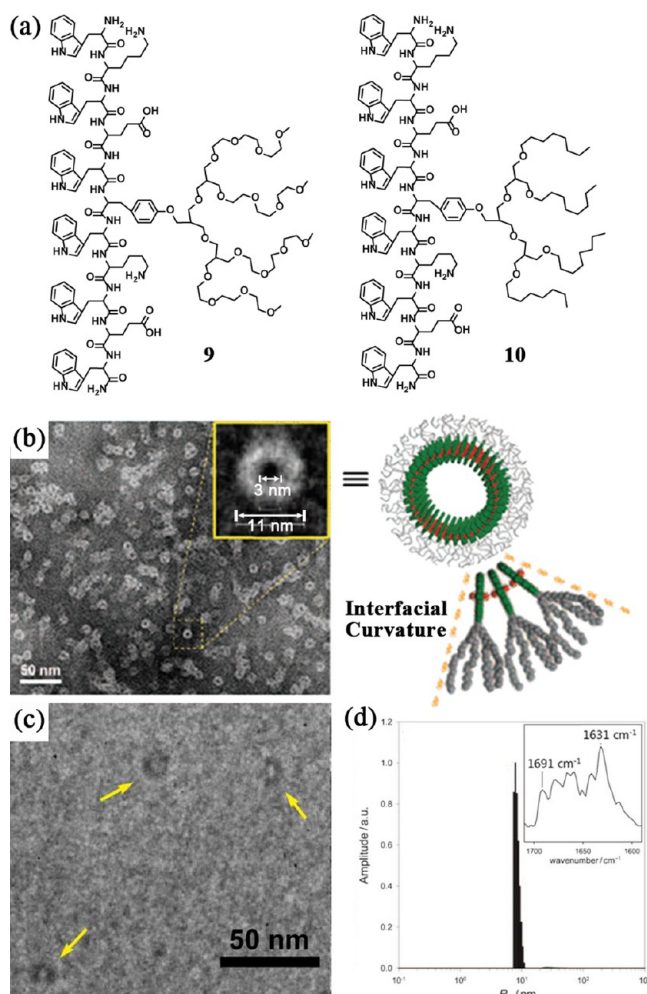
FIGURE 8. (a) Schematic structure of organic/peptide hybrid T-shape molecules **9** and **10**. (b) Negative-stained TEM image and (c) cryo-TEM image of peptide **9** in 20 mM KF aqueous solution and model of self-assembled toroidal nanostructure. (d) DLS data and FT-IR spectrum (inset) of **9**. Reprinted with permission from ref 52. Copyright 2011 John Wiley and Sons.

and a crossover point at 203 nm (Figure 9a, closed circle). To investigate the potential as transmembrane channels in the lipid bilayer, we performed a black lipid membrane experiment. A step-change behavior was obtained at an applied voltage of +40 mV across the membrane separating 1 M KCl, suggesting strong evidence of a single-ion channel (Figure 9b). The current (*I*)/voltage (*V*) plot in Figure 9c revealed that the ion channel formed by the peptide **10** showed an ohmic behavior, and a single-channel conductance of 263 pS was calculated from the slope for symmetrical 1 M KCl. The Hille equation for the single-channel conductance estimated the inner-channel diameter, $d_{Hille} \approx$ 0.5 nm, which showed contraction compared with inner diameter of toroids from **10**. Furthermore, an ion-transport assay with a small unilamellar vesicle (SUV) and pH-sensitive
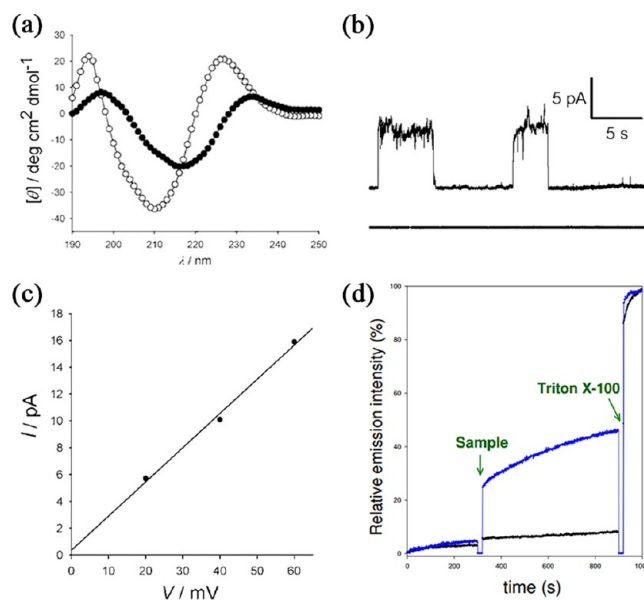

FIGURE 9. (a) (○) CD spectrum of **10** (20 μM in methanol); (●) CD spectrum of **10** in DOPC liposome (20 μM in water). (b) Current profile measured with and without **10** at +40 mV in 1 M KCl. (c) Single-channel *I*−*V* profile of conductance of **10** with a linear curve fit. (d) Liposome ion transport assay: (blue) changes in fluorescence intensity of intravesicular HPTS after addition of peptide **10** (5 μM); (black) a negative control experiment. Reprinted with permission from ref 52. Copyright 2011 John Wiley and Sons.

HPTS could suggest that **10** can form the pore in the membrane. When **10** was added at the indicated time point (300 s), the gradual signal of ion transport across the membrane was detected by the increase in relative fluorescence that accompanied the rise in intravesicular pH (Figure 9d). From all of these observations, we could speculate carefully that the toroidal nanostructure is formed from **10** and is incorporated into the lipid membrane, showing the transport activity of ions through its pore. However, because another model such as membrane leakage caused by **10** can be possible to explain its membrane activity, we will confirm the existence of the toroidal nanostructures on the membrane surface in further study.

Conclusions

Nanostructures and nanomaterials have been an interesting research field due to their application potential that ranges from electronic and detection materials to biomaterials. Nanostructures exhibit significantly different properties that depend on their physicochemical parameters, such as size, morphology, and stability. Among the many kinds of nanostructures, toroidal nanostructures have a unique symmetrical and annular shape similar to transmembrane protein shapes such as β-barrel and α-helical bundle. The work

described in this Account suggested that self-assembly of rigid−flexible amphiphiles and synthetic peptide-based amphilphiles can be attractive for generating highly defined toroidal nanostructures. The formation of curvature at the interface of building blocks or the stacking of the macrocycles can become the guiding principles for the construction of toroids. A few toroids showed activity as artificial transmembrane channels in a lipid bilayer through the toroidal model or the barrel−stave model, although the activity study was in the primary stage and should require more detailed research on the mechanism. Ultimately, this study has described a guiding approach to the development of toroidal nanostructures by self-assembly through rationally designed amphiphiles. We believe that the toroidal nanostructure can provide a fundamental understanding for the development of synthetic artificial transmembrane channels.

ABBREVIATIONS

TEM, transmission electron microscopy; cryo-TEM, cryogenic transmission electron microscopy; DLS, dynamic light scattering; AFM, atomic force microscopy; PEG, poly-(ethylene glycol); EYPC, egg-yolk phosphatidylcholine; PBS, phosphate-buffered saline; HPTS, 8-hydroxypyrene-1,3,6-trisulfonic acid; FT-IR, Fourier transform infrared; CD, circular dichroism; DOPC, dioleoylphosphatidylcholine;

BIOGRAPHICAL INFORMATION

Yongju Kim graduated from Seoul National University, Korea, with B.S. and Ph.D. degrees in chemistry in 2005 and 2012, respectively. His thesis focused on the development and construction of a chemical library for biological functions. In 2012, he joined Prof. Myongsoo Lee's National Creative Research Initiative Center for Supramolecular Nano-Assembly in a postdoctoral position. Then, he moved to Jilin University and joined Prof. Myongsoo Lee's group in 2013. His research interests are the synthesis and development of self-assembling molecules based on the synthetic rigid−flexible amphiphiles and peptide molecules to apply to biological systems.

Wen Li was born in 1980 in Inner Mongolia, China. He received his Ph.D. degree (2006) in chemistry from Jilin University, under the supervision of Prof. Lixin Wu. He did postdoctoral research with Prof. Myongsoo Lee at Seoul National University. He is currently an associated professor in Jilin University. His current research interests are the development of self-assembly structures based on clusto-supramolecular complexes and peptide block molecules.

Suyong Shin received her B.S. degree in chemistry from Ewha Womans University, Korea, in 2012 and now is a third semester graduate student pursuing her Ph.D. degree at Seoul National University. Her current research focus lies in the development of stimuli-responsive self-assembling nanostructures by using coordination interaction and supramolecular assembly.

Myongsoo Lee received a bachelor degree in Chemistry from Chungnam National University, Korea, in 1982 and his Ph.D. degree in Macromolecular Science from Case Western Reserve University in 1993. After a short postdoctoral appointment at University of Illinois at Urbana−Champaign, he joined the Faculty of Chemistry at Yonsei University (1994) and Seoul National University (2009), and then moved to Jilin University in 2013, where he is presently "Tang Au-Chin" Distinguished Professor of Chemistry. In 2002, he became a director of National Creative Research Initiative Center for Supramolecular Nano-Assembly. He received the PSK−Wiley Polymer Science Award for Young Scientist (2001), Yonsei Academy Award (2003), Scientist Award of This Month, Korea Ministry of Science & Technology (2006), Samsung Polymer Science Award (2008), and KCS Academy Award (2009). His main research interests include self-assembling molecules, controlled supramolecular structures, and peptide assembly.

FOOTNOTES

*Corresponding Author. E-mail: mslee@jlu.edu.cn.
The authors declare no competing financial interest.

REFERENCES

1 Aida, T.; Meijer, E. W.; Stupp, S. I. Functional supramolecular polymers. *Science* **2012**, *335*, 813–817.

2 Brunsveld, L.; Folmer, B. J. B.; Meijer, E. W.; Sijbesma, R. P. Supramolecular polymers. *Chem. Rev.* **2001**, *101*, 4071–4098.

3 Shimizu, T.; Masuda, M.; Minamikawa, H. Supramolecular nanotube architectures based on amphiphilic molecules. *Chem. Rev.* **2005**, *105*, 1401–1444.

4 Lim, Y.-b; Moon, K. S.; Lee, M. Recent advances in functional supramolecular nanostructures assembled from bioactive building blocks. *Chem. Soc. Rev.* **2009**, *38*, 925–934.

5 Ajayaghosh, A.; Praveen, V. K. π-Organogels of self-assembled p-phenylenevinylenes: Soft materials with distinct size, shape, and functions. *Acc. Chem. Res.* **2007**, *40*, 644–656.

6 Palmer, L. C.; Stupp, S. I. Molecular self-assembly into one-dimensional nanostructures. *Acc. Chem. Res.* **2008**, *41*, 1674–1684.

7 Wang, C.; Wang, Z.; Zhang, X. Amphiphilic building blocks for self-assembly: From amphiphiles to supra-amphiphiles. *Acc. Chem. Res.* **2012**, *45*, 608–618.

8 Zastavker, Y. V.; Asherie, N.; Lomakin, A.; Pande, J.; Donovan, J. M.; Schnur, J. M.; Benedek, G. B. Self-assembly of helical ribbons. *Proc. Natl. Acad. Sci. U. S. A.* **1999**, *96*, 7883–7887.

9 Yan, D.; Zhou, Y.; Hou, J. Supramolecular self-assembly of macroscopic tubes. *Science* **2004**, *303*, 65–67.

10 Engelkamp, H.; Middelbeek, S.; Nolte, R. J. M. Self-assembly of disk-shaped molecules to coiled-coil aggregates with tunable helicity. *Science* **1999**, *284*, 785–788.

11 Kim, J.-K.; Lee, E.; Kim, M.-C.; Sim, E.; Lee, M. Reversible transformation of helical coils and straight rods in cylindrical assembly of elliptical macrocycles. *J. Am. Chem. Soc.* **2009**, *131*, 17768–17770.

12 Hartgerink, J. D.; Beniash, E.; Stupp, S. I. Self-assembly and mineralization of peptide-amphiphile nanofibers. *Science* **2001**, *294*, 1684–1688.

13 Huang, Z.; Lee, H.; Lee, E.; Kang, S.-K.; Nam, J.-M.; Lee, M. Responsive nematic gels from the self-assembly of aqueous nanofibers. *Nat. Commun.* **2011**, *2*, No. 459.

14 Lee, E.; Kim, J.-K.; Lee, M. Reversible scrolling of two-dimensional sheets from the self-assembly of laterally grafted amphiphilic rods. *Angew. Chem., Int. Ed.* **2009**, *48*, 3657–3660.

15 Lim, Y.; Lee, E.; Lee, M. Toroidal nanostructures from self-assembly of block copolypeptides based on poly (l-arginine) and β-sheet peptide. *Macromol. Rapid Commun.* **2011**, *32*, 191–196.

16 Lim, Y.; Lee, M. Toroidal β-barrels from self-assembling β-sheet peptides. *J. Mater. Chem.* **2011**, *21*, 11680–11685.

17 Wimley, W. C. The versatile β-barrel membrane protein. *Curr. Opin. Struct. Biol.* **2003**, *13*, 404–411.

18 Walian, P.; Cross, T. A.; Jap, B. K. Structural genomics of membrane proteins. *Genome Biol.* **2004**, *5*, No. 215.

19 Jain, S.; Bates, F. S. On the origins of morphological complexity in block copolymer surfactants. *Science* **2003**, *300*, 460–464.

20 Pochan, D. J.; Chen, Z.; Cui, H.; Hales, K.; Qi, K.; Wooley, K. L. Toroidal triblock copolymer assemblies. *Science* **2004**, *306*, 94–97.

21 Huang, H.; Chung, B.; Jung, J.; Park, H.-W.; Chang, T. Toroidal micelles of uniform size from diblock copolymers. *Angew. Chem., Int. Ed.* **2009**, *48*, 4594–4597.

22 Butterfield, S. M.; Lashuel, H. A. Amyloidogenic protein–membrane interactions: Mechanistic insight from model systems. *Angew. Chem., Int. Ed.* **2010**, *49*, 5628–5654.

23 Djalali, R.; Samson, J.; Matsui, H. Doughnut-shaped peptide nano-assemblies and their applications as nanoreactors. *J. Am. Chem. Soc.* **2004**, *126*, 7935–7939.

24 Yagai, S.; Mahesh, S.; Kikkawa, Y.; Unoike, K.; Karatsu, T.; Kitamura, A.; Ajayaghosh, A. Toroidal nanoobjects from rosette assemblies of melamine-linked oligo(p-phenyleneethynylene)s and cyanurates. *Angew. Chem., Int. Ed.* **2008**, *47*, 4691–4694.

25 Carlson, J. C. T.; Jena, S. S.; Flenniken, M.; Chou, T.-f.; Siegel, R. A.; Wagner, C. R. Chemically controlled self-assembly of protein nanorings. *J. Am. Chem. Soc.* **2006**, *128*, 7630–7638.

26 Lee, M.; Cho, B.-K.; Zin, W.-C. Supramolecular structures from rod–coil block copolymers. *Chem. Rev.* **2001**, *101*, 3869–3892.

27 Kim, H.-J.; Kim, T.; Lee, M. Responsive nanostructures from aqueous assembly of rigid–flexible block molecules. *Acc. Chem. Res.* **2011**, *44*, 72–82.

28 Lee, E.; Kim, J.-K.; Lee, M. Tubular stacking of water-soluble toroids triggered by guest encapsulation. *J. Am. Chem. Soc.* **2009**, *131*, 18242–18243.

29 Kim, H.-J.; Kang, S. K.; Lee, Y. K.; Seok, C.; Lee, J. K.; Zin, W. C.; Lee, M. Self-dissociating tubules from helical stacking of noncovalent macrocycles. *Angew. Chem., Int. Ed.* **2010**, *49*, 8471–8475.

30 Huang, Z.; Kang, S.-K.; Banno, M.; Yamaguchi, T.; Lee, D.; Seok, C.; Yashima, E.; Lee, M. Pulsating tubules from noncovalent macrocycles. *Science* **2012**, *337*, 1521–1526.

31 Percec, V.; Dulcey, A. E.; Balagurusamy, V. S. K.; Miura, Y.; Smidrkal, J.; Peterca, M.; Nummelin, S.; Edlund, U.; Hudson, S. D.; Heiney, P. A. Self-assembly of amphiphilic dendritic dipeptides into helical pores. *Nature* **2004**, *430*, 764–768.

32 Ghadiri, M. R.; Granja, J. R.; Milligan, R. A.; McRee, D. E.; Khazanovich, N. Self-assembling organic nanotubes based on a cyclic peptide architecture. *Nature* **1993**, *366*, 324–327.

33 Valéry, C.; Paternostre, M.; Robert, B.; Gulik-Krzywicki, T.; Narayanan, T.; Dedieu, J.-C.; Keller, G.; Torres, M.-L.; Cherif-Cheikh, R.; Calvo, P. Biomimetic organization: Octapeptide self-assembly into nanotubes of viral capsid-like dimension. *Proc. Natl. Acad. Sci. U. S. A.* **2003**, *100*, 10258–10262.

34 Kim, H. S.; Hartgerink, J. D.; Ghadiri, M. R. Oriented self-assembly of cyclic peptide nanotubes in lipid membranes. *J. Am. Chem. Soc.* **1998**, *120*, 4417–4424.

35 Futaki, S. Peptide ion channels: Design and creation of function. *Pept. Sci.* **1998**, *47*, 75–81.

36 Lashuel, H. A.; Hartley, D.; Petre, B. M.; Walz, T.; Lansbury, P. T. Neurodegenerative disease: amyloid pores from pathogenic mutations. *Nature* **2002**, *418*, 291–291.

37 Lim, Y.-b.; Moon, K.-S.; Lee, M. Stabilization of an α-helix by β-sheet-mediated self-assembly of a macrocyclic peptide. *Angew. Chem., Int. Ed.* **2009**, *48*, 1601–1605.

38 Matile, S. En route to supramolecular functional plasticity: Artificial β-barrels, the barrel-stave motif, and related approaches. *Chem. Soc. Rev.* **2001**, *30*, 158–167.

39 Sisson, A. L.; Shah, M. R.; Bhosale, S.; Matile, S. Synthetic ion channels and pores (2004–2005). *Chem. Soc. Rev.* **2006**, *35*, 1269–1286.

40 Fyles, T. M. Synthetic ion channels in bilayer membranes. *Chem. Soc. Rev.* **2006**, *36*, 335–347.

41 Matile, S.; Vargas Jentzsch, A.; Montenegro, J.; Fin, A. Recent synthetic transport systems. *Chem. Soc. Rev.* **2011**, *40*, 2453–2474.

42 Chui, J. K. W.; Fyles, T. M. Ionic conductance of synthetic channels: analysis, lessons, and recommendations. *Chem. Soc. Rev.* **2012**, *41*, 148–175.

43 Sakai, N.; Mareda, J.; Matile, S. Rigid-rod molecules in biomembrane models: From hydrogen-bonded chains to synthetic multifunctional pores. *Acc. Chem. Res.* **2005**, *38*, 79–87.

44 Sakai, N.; Mareda, J.; Matile, S. Artificial β-barrels. *Acc. Chem. Res.* **2008**, *41*, 1354–1365.

45 Kaucher, M. S.; Peterca, M.; Dulcey, A. E.; Kim, A. J.; Vinogradov, S. A.; Hammer, D. A.; Heiney, P. A.; Percec, V. Selective transport of water mediated by porous dendritic dipeptides. *J. Am. Chem. Soc.* **2007**, *129*, 11698–11699.

46 Fyles, T. M.; Hu, C. W.; Luong, H. Solid-phase synthesis of oligoester ion channels. *J. Org. Chem.* **2006**, *71*, 8545–8551.

47 Fyles, T. M.; Luong, H. Structure–activity relationships in linear oligoester ion-channels. *Org. Biomol. Chem.* **2009**, *7*, 733–738.

48 Moszynski, J. M.; Fyles, T. M. Synthesis, transport activity, membrane localization, and dynamics of oligoester ion channels containing diphenylacetylene units. *Org. Biomol. Chem.* **2010**, *8*, 5139–5149.

49 Brogden, K. A. Antimicrobial peptides: Pore formers or metabolic inhibitors in bacteria? *Nat. Rev. Microbiol.* **2005**, *3*, 238–250.

50 Jang, H.; Zheng, J.; Lal, R.; Nussinov, R. New structures help the modeling of toxic amyloidβ ion channels. *Trends Biochem. Sci.* **2008**, *33*, 91–100.

51 Yang, W. Y.; Ahn, J. H.; Yoo, Y. S.; Oh, N. K.; Lee, M. Supramolecular barrels from amphiphilic rigid–flexible macrocycles. *Nat. Mater.* **2005**, *4*, 399–402.

52 Park, I. S.; Yoon, Y. R.; Jung, M.; Kim, K.; Park, S. B.; Shin, S.; Lim, Y.; Lee, M. Designer nanorings with functional cavities from self-assembling β-sheet peptides. *Chem.—Asian J.* **2011**, *6*, 452–458.